ACS OMEGA

http://pubs.acs.org/journal/acsodf

Article

Continuous-Flow Ammoxidation of 2-Methylpyrazine to 2-Cyanopyrazine with High Space-Time Yield in a Microreactor

Meixiu Wei, Haoran Ma, Qilin Lu, Da Ruan, Zhengdong Ma, and Xiao Chen*

Cite This: *ACS Omega* 2022, 7, 8980−8987

Read Online

ACCESS | Metrics & More | Article Recommendations | Supporting Information

ABSTRACT: A microreactor (MR) with a vaporization microchamber and a sinusoidal wave microchannel was fabricated to synthesize 2-cyanopyrazine (CP) directly with an aqueous 2-methylpyrazine (MP) solution. A continuous-flow process with high space-time yield was achieved under the premise of strong exothermality of this ammoxidation reaction. The vanadium metal oxide catalysts with four different supports (α-Al_2O_3, γ-Al_2O_3, ZSM-5(50), ZSM-5(80)) were evaluated by simply stacking in the wave microchannel from 350 to 540 °C. The process parameters (temperature, reactant ratio, and size of catalysts) were optimized with the selected CrVPO/γ-Al_2O_3 catalyst, and an optimal ammoxidation process with MP conversion (X_{MP}) of 71.5% and CP selectivity (S_{CP}) of 93.7% was obtained by a volume space velocity (GHSV) of 13 081 h^{-1} at 480 °C. Correspondingly, the space-time yield of CP (STY_{CP}) was 1724−77 082 $g_{CP}kg_{cat}^{-1}h^{-1}$, which was the highest value ever reported for this reaction. Meanwhile, the ammoxidation reaction showed a great continuous-synthesis stability of 50-h running in the microreactor with the CP yield (Y_{CP}) remaining 56%−68%.

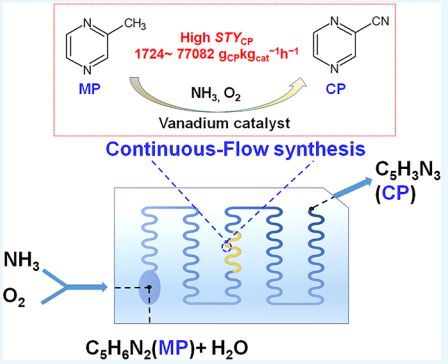

1. INTRODUCTION

Heterogeneous catalytic ammoxidation of alkyl aromatics and heteroaromatics is an essential reaction to synthesize a variety of pharmaceutical and chemical products, characterized by the conversion of methyl to nitrile group.[1,2] Some bulk-chemical-product reactions, like propylene to acrylonitrile,[3−6] propane to acrylonitrile,[7−10] ethane ammoxidation to acetonitrile and ethylene,[11−13] have been researched extensively and deeply since the 1970s. However, because of the strong exothermic characteristics of the ammoxidation reaction, efficient heat-transfer and intrinsic-safety had been mainly focused even to now.[14] Additionally, pharmaceutical-product reactions, like ammoxidation of 2-methylpyrazine (MP) to 2-cyanopyrazine (CP), which now is a chosen low cost and short-path route to synthesize antituberculosis (TB) drug pyrazinamide,[3] have attracted gradually increasing attention (Scheme 1).

At present, MP ammoxidation research mainly focuses on catalysts.[15−24] Mixed oxide catalysts (MV, M = Al, Fe, Cr, Nb, La, Bi, La)[19,20,23] at 320−460 °C, supported vanadium metal oxide catalysts (V_2O_5−Au/TiO, CrVPO/Al_2O_3)[21,17] at 370−400 °C, and metal-salt catalysts[15,16,18,22,24] at about 450 °C had been investigated, and the reported CP yield were 50−86%. Among these catalysts, CrVPO was more promising by its lower cost and better performance of >85% yield and 92% selectivity.[17] To be mentioned, the highest space-time yield (STY) of CP were reported as 500−900 $g_{CP}{\cdot}kg_{cat}^{-1}{\cdot}h^{-1}$ by a $La_{0.1}V_{0.9}O_x$ catalyst in 2016.[23]

In recent years, microreactors[25−30] had been applied for the ammoxidation reaction,[31,32] like from propane to acrylonitrile, and showed good performance by its high heat transfer coefficient. However, the reported MP ammoxidation mainly used Φ20−30 mm fixed-bed reactors (FBR), and the reaction temperature was limited within 450 °C because of possible hot spots at higher temperature. Especially, when the flow rate of MP was high in a FBR reactor, the expansion of hot spots in the catalyst bed might increase byproducts of carbon oxides and reduce the yield of CP.[23] With respect to the results of higher reaction temperature can raise the MP conversion and may be tolerated by the microreactor,[33−38] obviously a continuous-flow microreactor carrying out MP ammoxidation stably at higher temperature would be an ideal reactor for efficiently synthesis CP. Especially, a continuous microfluidic flow would imbue an improved safety profile through the use

Scheme 1. Reaction Scheme for Ammoxidation of MP[a]

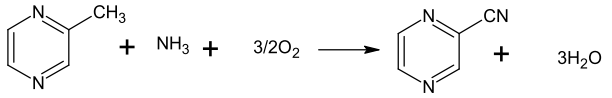

[a]The reaction leads to CP, other heteroaromatic byproducts, and products of total oxidation as well.

Received: January 3, 2022
Accepted: February 23, 2022
Published: March 2, 2022

of reduced volumes of gas within limited explosion space, which is also called the intrinsic safety of microreactors. Therefore, a continuous-flow microreaction may be feasible to get an integration solution of temperature control of MP ammoxidation and CP STY improvement.

In this study, we designed and fabricated a microreactor with a vaporization microchamber and a sinusoidal wave microchannel, aiming to synthesize CP by ammonia oxidation at high temperature under continuous gas−liquid mixture feeding. The performance of this microreactor was systematically studied with CrVPO as the catalyst.

2. EXPERIMENTAL SECTION

2.1. Materials. Chromium trioxide (AR) was purchased from Chengdu Jinshan Chemical Reagent Co. Ltd. Vanadium pentoxide (AR) was purchased from Tianjin Meilin Industry and Trade Co. Ltd. Phosphoric acid (AR) was purchased from Chengdu Kelong Chemical Reagent Factory. Oxalic acid was purchased from Tianjin Zhiyuan Chemical Reagent Co. Ltd. 2-Methylpyrazine (AR) and other chemicals used in this work were obtained from Chengdu Best Reagent Co. Ltd. All the chemicals were used as purchased without any further purification.

2.2. Fabrication of Microreactor. Figure 1 is the schematic diagram of the microreactor, which consists of a

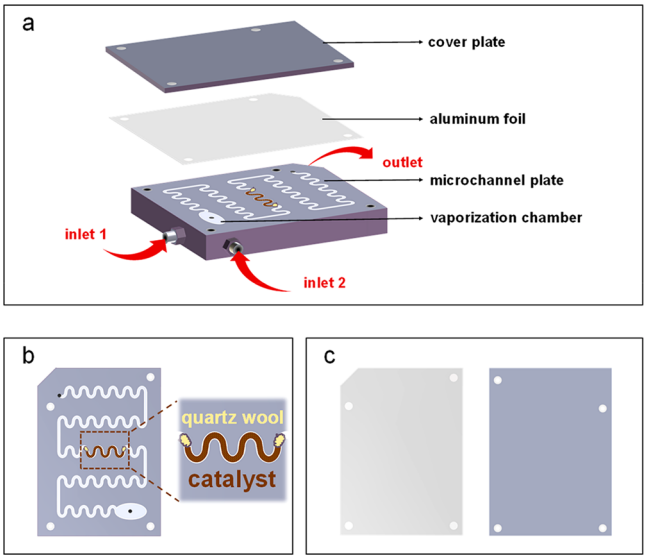

Figure 1. Schematic diagram of the microreactor (a) and details of the microchannel plate and the catalyst packing method (b), aluminum foil, and cover plate (c).

stainless steel microchannel plate (Figure 1b), aluminum foil, and a cover plate (Figure 1c). The microreactor was assembled by laminating the three plates with bolts. The microchannel was machined out on the 20 mm-in-depth stainless steel plate and made up of two sections: an elliptical liquid vaporization chamber and a sinusoidal wave microchannel. The former was with a long axis of 20 mm and a short axis of 10 mm. The latter was with a width and height of 2.0 mm and 0.5 mm, respectively. The total length of the microchannel is 440 mm. The liquid vaporization chamber was designed to realize vaporization, mixing, and heat transfer simultaneously. The reactant inlet was connected with the chamber, which provides expansion space for the vaporization of MP solution, reduces the gas velocity, and prolongs the mixing time with other gas feeds. Moreover, the sinusoidal wave microchannel was utilized to constantly redirect the gas fluid and promote micromixing.[39] The sinusoidal structure design could also reduce the dead angle, which is conducive to the cleaning and reuse of the microreactor. A 0.1 mm thick aluminum foil was added as the O-seal between the microchannel plate and the cover. The good ductility and heat resistance of aluminum foil enhanced channel encapsulation under high-temperature conditions and improved the airtightness of the device.

2.3. Preparation of CrVPO Catalysts. The CrVPO catalyst was prepared with the impregnation method.[11] First, 2.7 g of oxalic acid, 0.284 g of vanadium pentoxide (V_2O_5), and 0.25 g of chromium trioxide (CrO_3) were successively dissolved in 35 mL of distilled water. Next, 0.275 mL of phosphoric acid (H_3PO_4) was added to get the molar ratio of Cr:V:P = 0.8:0.5:1.7, and then the mixture was stirred at a constant temperature of 50−70 °C for 10 min. When the solution was cooled to room temperature, 2.5 g of catalyst support (α-Al_2O_3, γ-Al_2O_3, ZSM-5(50), ZSM-5(80), here 50 and 80 refer to the Si/Al ratio of the ZSM-5 molecular sieve) was added into the solution and shaken at 80 rpm for 24−48 h in an immersion oscillator (SHZ−B, Jintan) after ultrasonic treatment at 50 W power for 6 h. The catalysts were formed by drying with rotary evaporation at 60 °C and calcination at 550 °C for 2 h. Finally, an agate mortar was used to grind the solid catalysts, and the powder was screened with sieves of 40−140 meshes.

2.4. Catalyst Tests. The performance of CrVPO catalysts in the microreactor was characterized by an experimental apparatus shown in Figure 2. First, the catalyst powder with 5 particle sizes from 0.1 mm to 0.4 mm was piled into the microgroove in the center of the microchannel plate, and quartz wool was placed on both sides of the catalyst section to prevent the catalyst from being carried out by the gas flow. Then the aluminum foil plate and the cover plate were installed according to the device diagram in Figure 1 and fastened with bolts. After that, a gas detector was used to test the airtightness of the assembled microreactor. If the tightness tests were passed, the reactor temperature would be raised to a certain degree in the N_2 atmosphere. After the required temperature was reached for at least 5 min, the ammoxidation reactions was started by precisely controlling the gas feed flow of NH_3 and O_2 with two mass flowmeters (D07-19, Sevenstar), and the flow of MP solution was controlled with a plunger pump (TBP-1002, Tauto Biotech). The temperature of the microreactor was detected and controlled by a temperature controller equipped with a 1500 W electric heater beneath the microchannel plate. Generally, the products were continuously collected at the outlet and detected every 5 min. Data were collected 5 times and then averaged.

The residence time τ and the volume space velocity (GHSV) were calculated to evaluate the reaction conditions using the following formulas:

$$\tau = \frac{V_{cat}}{\nu_{total}} \quad (1)$$

$$\mathrm{GHSV} = \frac{\nu_{total}}{V_{cat}} \quad (2)$$

where V_{cat} was the volume of catalyst loading in the microchannels, and ν_{total} was volume flow rate of total gas reactants at the inlet of the microreactor.

https://doi.org/10.1021/acsomega.2c00039
ACS Omega 2022, 7, 8980−8987

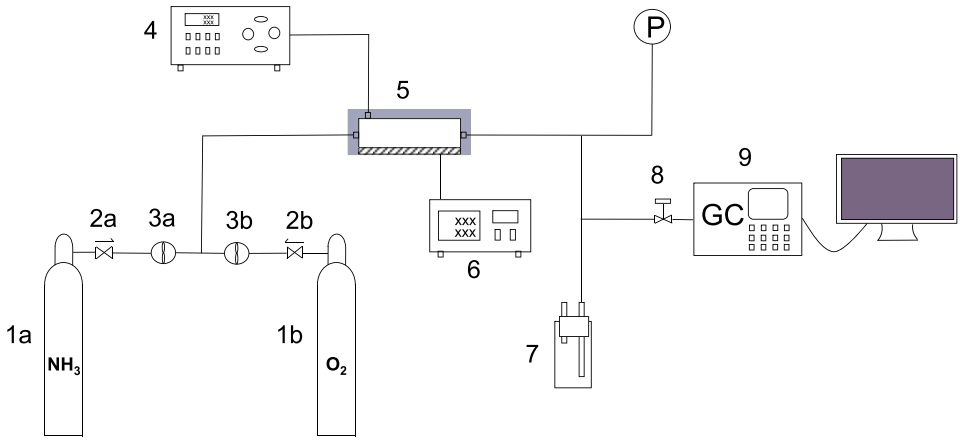

Figure 2. Schematic diagram of apparatus. 1, cylinder; 2, relief valve; 3, mass flowmeter; 4, plunger pump; 5, microreactor; 6, temperature controller; 7, absorber bottle; 8, off valve; 9, gas chromatograph.

The product samples were analyzed with gas chromatography (SC-3000B, Chuanyi) by the internal standard method when the continuous reaction got a steady state. The GC condition was as follows: hydrogen flame ionization detector, BK-wax capillary column 30 m × 0.32 mm × 0.5 μm). Oven temperature: 120−180 °C; detector temperature: 220 °C; vaporization chamber temperature: 220 °C; oven heating program setting: heating from 120 to 180 °C, heating at a rate of 20 °C/min, at 180 °C, The column oven temperature was constant for 2 min; carrier gas nitrogen (N_2): 0.4 mL/s, hydrogen (H_2): 0.5 mL/s; air: 1.5 mL/s; precolumn pressure: 0.2 MPa; injection volume: 0.4 μL; Injection mode: split injection; split ratio: 30:1; makeup gas: N_2: 0.4 mL/s. During 50 h of stability tests, product samples were collected every 6 h in a steady state after 2 h of reaction.

The conversion of MP (X_{MP}), the yield and the selectivity of CP (Y_{CP}, S_{CP}), and MP-based space-time yield (STY_{CP}) were calculated using the following formulas:

$$X_{MP} = \frac{c_{MP,0} - c_{MP}}{c_{MP,0}} \quad (3)$$

$$Y_{CP} = \frac{c_{CP}}{c_{MP,0}} \quad (4)$$

$$S_{CP} = \frac{c_{CP}}{c_{MP,0} - c_{MP}} \quad (5)$$

$$STY_{CP} = \frac{F_{MP,0} \times Y_{CP} \times M_{CP}}{m_{cat}} \quad (6)$$

where $c_{MP,0}$ and c_{MP} were the MP concentration at the inlet and outlet of the microreactor respectively, c_{CP} was the CP concentration at the outlet, $F_{MP,0}$ was the molar flow rate of MP at the inlet, M_{CP} was the molar mass of CP and m_{cat} is the mass of the catalyst used.

3. RESULTS AND DISCUSSION

3.1. Catalytic Performance of Four Catalysts. With respect to the process, the catalytic reaction needs to endure microfludic operation conditions in the microreator, like enhanced mass transfer, high gas velocity, and so on. Therefore, to screen the optimal catalyst for the microreaction of ammoxidation, four kinds of supports (α-Al_2O_3, γ-Al_2O_3, ZSM-5(50), ZSM-5(80)) were evaluated for the CrVPO catalyst at 480 °C, and the feed molar ratio is 1:5:6:12 ($MP:H_2O:NH_3:O_2$). The results are shown in Figure 3. The

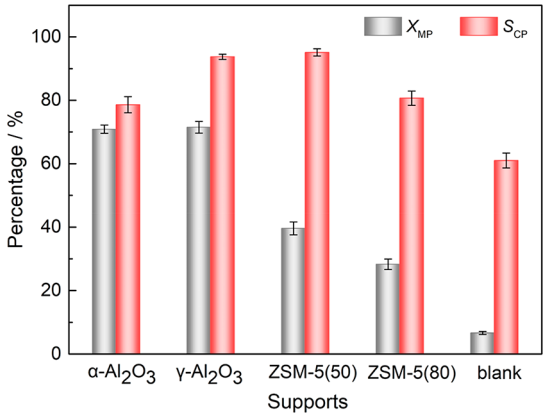

Figure 3. Effects of different supports on the CP synthesis (reaction conditions: T = 480 °C; feed molar ratio: $MP:H_2O:NH_3:O_2$ = 1:5:6:12; catalyst weight = 0.03 g; MP flow: 0.05 mL/min, NH_3 flow: 75 mL/min, O_2 flow: 150 mL/min).

results showed that the selectivity of CP reached over 90% on CrVPO/γ-Al_2O_3 and CrVPO/ZSM-5 (50); the best conversion of MP reached 71.5% on CrVPO/γ-Al_2O_3; and the blank showed the lowest conversion (X_{MP} = 7.4%). Additionally, CrVPO/γ-Al_2O_3 was chosen as the optimal catalyst for its best MP conversion and high CP selectivity. Notably, the above performances were achieved under a microfludic operation conditions, in which the load mass of catalyst was only 0.03 g and the residence time in the microreactor was as short as <0.01 s. As a comparison, the corresponding conditions were 1−3 g catalyst load and ∼1 s resident time in the conventional FBR, which were nearly 2 orders of magnitude higher. Obviously, the reaction productivity of MP ammoxidation got enhanced in the microreactor with much higher volume space velocity and space-time yield of CP, and both parameters will be discussed in detail later.

3.2. Characterization of Catalysts. To indicate the suitable catalyst structure for the microreaction, the micromorphology, surface area, and element distribution of the catalysts were characterized with SEM (JSM 7160F, JEOL), BET (VII 2390, Gemini), and EDS (Ultim Max65), and the

https://doi.org/10.1021/acsomega.2c00039
ACS Omega 2022, 7, 8980−8987

results are shown in Figure 4, Table 1, and Figure 5, respectively.

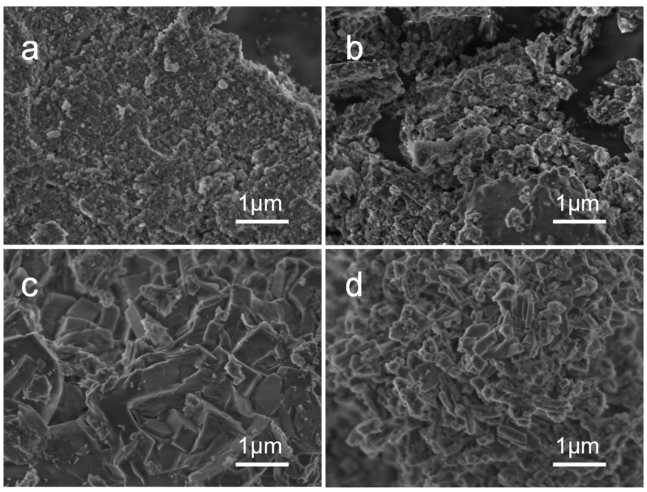

Figure 4. SEM images of CrVPO loaded with γ-Al_2O_3 by the impregnation method (a) and α-Al_2O_3 (b), ZSM-5(50) (c), and ZSM-5(80) (d).

Table 1. Properties of Different Samples

entry	sample	surface area (m^2/g)[a]	pore volume (cc/g)[b]	pore size (nm)
1	CrVPO/γ-Al_2O_3	121.72	0.23	8.67
2	CrVPO/α-Al_2O_3	29.72	0.12	21.53
3	CrVPO/ZSM-5(50)	244.29	0.11	9.39
4	CrVPO/ZSM-5(80)	290.04	0.13	12.48

[a]Determined by N_2 adsorption/desorption using the Brunauer–Emmett–Teller (BET) method. [b]Determined by Barrett–Joyner–Halenda (BJH) method.

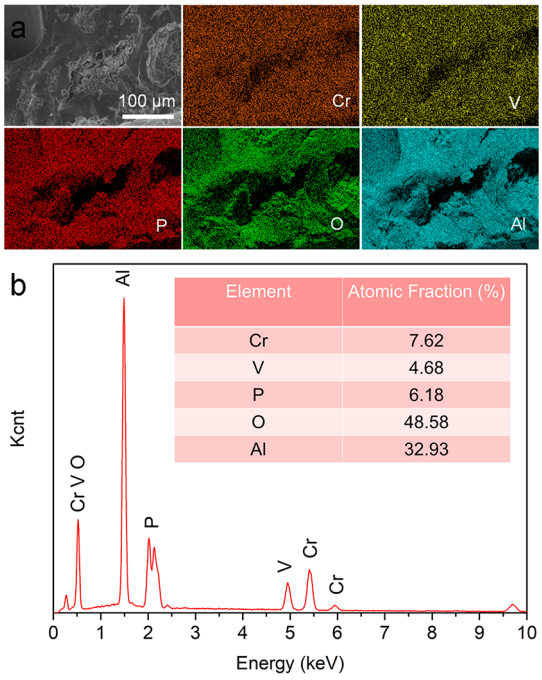

Figure 5. SEM images and EDS surface scan of the cross section of CrVPO/γ-Al_2O_3 catalyst (a) and atomic fraction of different elements on the catalyst (b).

As shown in Figure 4a,b, the CrVPO/γ-Al_2O_3 sample (panel a) and the CrVPO/α-Al_2O_3 sample (panel b) had typical particle–substrate structures. As shown in Figure 4c,d, respectively, the CrVPO/ZSM-5(50) sample (panel c) and the CrVPO/ZSM-5(80) sample (panel d) had relatively uniform particle-packing structures. From the comparison of the four catalysts, obviously CrVPO/α-Al_2O_3 (Figure 4b) had the biggest bare substrate, CrVPO/ZSM-5(80) (Figure 4d) had the smallest packing particles; however, both CrVPO/γ-Al_2O_3 (Figure 4a) and CrVPO/ZSM-5(50) (Figure 4c) apparently have moderately stacked structures. The BET analyses in Table 1 proved that the smallest pore size of ~9 nm was presented by the catalyst of CrVPO/γ-Al_2O_3 and CrVPO/ZSM-5, which may be the reason for best catalytic performance of CP selectivity. However, the relationship between catalyst performance and surface area had no obvious correlation, and the CrVPO/γ-Al_2O_3 with biggest MP conversion only had the medium surface area of 121.72 $m^2 \cdot g^{-1}$. Compared with the surface area of pure γ-Al_2O_3 (ca. 190 $m^2 \cdot g^{-1}$), the surface area of CrVPO/γ-Al_2O_3 decreased obviously, which should be caused by the loading of active CrVPO components. The corresponding N_2 adsorption–desorption isotherms are shown in Figure S1.

Figure 5 showed the EDS elemental analysis on the cross section of the best catalyst CrVPO/γ-Al_2O_3. As observed in Figure 5a, Cr, P, and V were well-dispersed in the catalyst inner pores, indicating that these active components were fully transferred and diffused into the γ-Al_2O_3 support inner surface after ultrasonic treated for 6 h and impregnated for at least 24 h. The atomic ratio of Cr, V, P, O, Al was 1:0.6:0.8:6.3:4.3 (Figure 5b). These active components on the support may provide a suitable dehydrogenation and oxygen supply center for the ammonia oxidation process, which could make the catalyst show good catalytic performance.

The effect of the immersion time and the catalyst size on the MP conversion and CP selectivity were also investigated, and the results are shown in Figures S2 and S3, alternatively. According to Figure S2, when the immersion time of the CrVPO/γ-Al_2O_3 catalyst increased from 24 to 72 h, the conversion of MP increased from 62.9% to 71.5% and then remained unchanged with the immersion time increase furthermore. In Figure S3, the yield of CP first increased as the catalyst particle size decreased. The highest conversion of MP was obtained when the catalyst particle size was between 0.15 and 0.18 mm.

3.3. Effect of Reaction Temperature. The effect of reaction temperature on the ammoxidation of MP was shown in Figure 6. The CP selectivity remained almost 90% in the temperature range from 350 to 540 °C. When the temperature was 350 °C, the conversion of MP was only 1.5%. As the reaction temperature increased, the conversion of MP increased rapidly. After the temperature reached 480 °C, the conversion increase slowed down, and the selectivity of CP decreased thereafter. At 480 °C, the CP selectivity was 93.7%, slightly higher than that at 460 and 500 °C, and the conversion of MP reached 71.5%.

To be mentioned, the reaction temperature in our microreactor was higher compared with the CP-synthesizing temperature range of 320–460 °C, which were generally employed in the traditional fixed-bed reactors by previous literature.[15,18–20,23] The MP ammoxidation reaction has violent exothermicity and easily explodes, and it is challenging to carry out the reaction stably at a higher temperature.

https://doi.org/10.1021/acsomega.2c00039
ACS Omega 2022, 7, 8980–8987

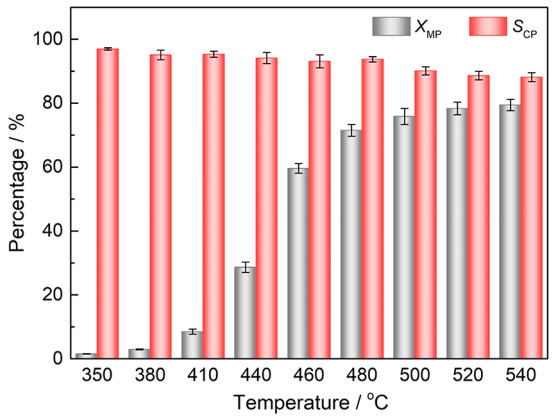

Figure 6. Effects of reaction temperature on the CP synthesis (reaction conditions: CrVPO/γ-Al_2O_3 catalyst; feed molar ratio: MP:H_2O:NH_3:O_2 = 1:5:6:12; τ = 0.004 s; m_{cat} = 0.03g; MP flow: 0.05 mL/min, NH_3 flow: 75 mL/min, O_2 flow: 150 mL/min).

However, during the two years of our research, the reaction temperature inside the microreactor usually varied within ±1 °C for a typical 5-h experiment. Obviously with the help of efficient heat transfer in the microspace, the ammoxidation from MP to CP could be easily run at a higher temperature in the specially designed microreactor.

3.4. Effect of Molar Ratio of MP to Water. For MP ammoxidation reactions in the conventional reactors, water vapor was essential to promote product desorption and control the exotherm.[11] Subsequently, the influence of water on the reaction efficiency was investigated with MP solutions of different concentrations (molar ratio of MP to water = 1:20, 1:7, 1:5, 1:3, 1:1) as the reactants. The results are shown in Figure 7. It could be found that with the increase of water in

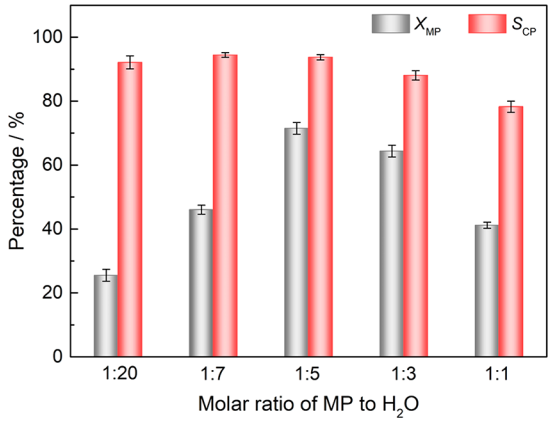

Figure 7. Influence of molar ratio of MP to water on the CP synthesis (reaction conditions: CrVPO/γ-Al_2O_3 catalyst; T = 480 °C; feed molar ratio: MP:H_2O:NH_3:O_2 = 1:x:6:12; τ = 0.004 s; m_{cat} = 0.03g; MP flow: 0.05 mL/min, NH_3 flow: 75 mL/min, O_2 flow: 150 mL/min).

the MP solution, the CP selectivity showed an obvious trend of first increasing and then decreasing, keeping above 90% when the molar ratios of MP to water were 1:20, 1:7, and 1:5. The MP conversion showed the same trend but reached a maximum value of 71.5% when the molar ratio was 1:5. It was concluded that appropriate addition of water could help to increase the MP conversion and the CP selectivity. Compared with the molar ratio of MP to water used in the traditional fixed-bed reactors,[11] the optimal ratio of 1:5 in this research was lower, which suggested that because of the higher reaction temperature and the better heat transfer in the microreactor, less water was needed for the product desorption and temperature control.

Moreover, the effect of ammonia consumption on the synthesis was investigated by varying the feed molar ratio of MP:H_2O:O_2:NH_3 = 1:5:12:x, taking x = 2, 4, 6, 8, 10. The result (refer to Figure S4) showed that excessive ammonia gas within a certain range could improve the MP conversion. The molar ratio of MP:ammonia of 1:6 was suitable for the continuous synthesis. The effect of oxygen consumption on the synthesis was investigated by varying the feed molar ratio of MP:H_2O:NH_3:O_2 = 1:5:6:x, with x = 8, 10, 12, 14, 16. It could be found in Figure S5 that when the oxygen molar ratio increased, the conversion first increased and then decreased. The optimal molar ratio of MP to oxygen is 1:12, obtaining the highest MP conversion of 71.5% and the best CP selectivity of 93.7%.

3.5. Volume Space Velocity. By varying the mass of the catalyst used in the MP ammoxidation reaction, the effect of volume space velocity GHSV on the CP yield was investigated, and the results are shown in Figure 8.

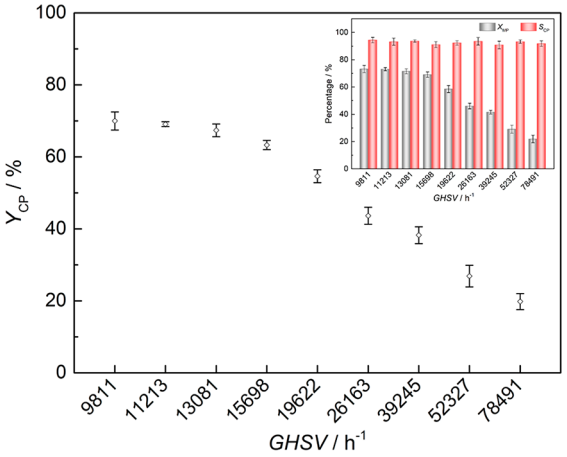

Figure 8. Effect of volume space velocity GHSV on the CP yield (reaction conditions: T = 480 °C; feed molar ratio: MP:H_2O:NH_3:O_2 = 1:5:6:12; τ = 0.001−0.005 s; m_{cat} = 0.005−0.04 g; MP flow: 0.05 mL/min, NH_3 flow: 75 mL/min, O_2 flow: 150 mL/min).

From Figure 8, it can be observed that the CP yield Y_{CP} decreased when GHSV increased from 9811 h^{-1} to 78 491 h^{-1}. When the catalyst mass was 0.04 g and GHSV was 9811 h^{-1}, the maximum reaction yield was 69.1%. However, the GHSV of 13 081 h^{-1}, corresponding to a catalyst mass of 0.03 g, obviously was the turning point after which the CP yield decreased sharply. From the relationship between MP conversion X_{MP}, CP selectivity S_{CP} and GHSV in the inset, it could be seen that the increase of GHSV leads to a decrease in X_{MP}, which was almost in sync with the trend in Y_{CP}. The GHSV is inversely proportional to the residence time τ. In Figure 8, τ had a small absolute value of only 0.001−0.005 s, and thus, S_{CP} did not change much. This result revealed that at a short τ less than 0.01 s, an increase in catalyst dosage was beneficial to improve the conversion and yield. Importantly, a lower mass of catalyst caused a lower CP yield, and excessive catalyst led to increasing pressure and gas obstruction. Therefore, the optimal catalyst mass chosen for this experi-

https://doi.org/10.1021/acsomega.2c00039
ACS Omega 2022, 7, 8980−8987

ment was 0.03 g, and the corresponding GHSV was 13 081 h^{-1}.

3.6. Stability. The reaction stability in the microreactor was explored with the continuous reaction, by using the obtained optimal conditions (CrVPO/γ-Al_2O_3 catalyst particle size 0.15−0.18 mm, catalyst mass 0.03 g, reaction temperature 480 °C, and feed molar ratio MP:H_2O:NH_3:O_2 = 1:5:6:12). The result was shown in Figure 9. It could be found that the microreactor could be operated stably for at least 50 h, and MP yield remains 56−68% for the whole continuous process. This result showed that the advantages of efficient reaction and sufficient heat removal could be maintained for the 50-h continuous reaction process and CP could be synthesized stably and efficiently in the microreactor.

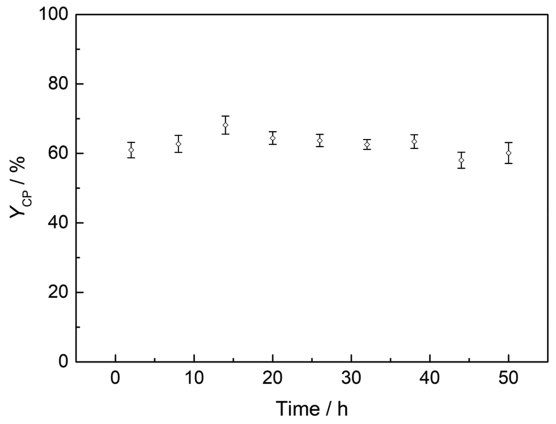

Figure 9. Reaction stability experiment in the miroreactor (reaction conditions: T = 480 °C; feed molar ratio: MP:H_2O:NH_3:O_2= 1:5:6:12; τ = 0.004 s; m_{cat} = 0.03 g; MP flow: 0.05 mL/min, NH_3 flow: 75 mL/min, O_2 flow: 150 mL/min).

3.7. Space-Time Yield. Many researchers had reported the ammoxidation of MP to CP in conventional fixed-bed reactors with different catalysts, and Table 2 compared these results and our result mainly focusing on the catalyst loading, the residence time, and the space-time yield. Compared to these investigations, a much shorter residence time (0.004 s) and less catalyst loading (0.03 g) were used in our microreactor. However, the microchannel reactor applied to the ammoxidation of MP has obtained a space-time yield of at least 1724 $g_{CP}kg_{cat}^{-1}h^{-1}$, which is nearly twice as large as the space-time yield of 440−900 $g_{CP}kg_{cat}^{-1}h^{-1}$ in the conventional fixed-bed reactor. And the highest space-time yield reached 77 082 $g_{CP}kg_{cat}^{-1}h^{-1}$ in this work. It was obvious that the ammoxidation from MP to CP could be much more efficiently carried out in the microreactor than in regular reactors.

4. CONCLUSIONS

The continuous-flow ammoxidation reaction of 2-methylpyrazine (MP) to 2-cyanopyrazine (CP) with high space-time yield was achieved at 350 °C ∼ 540 °C by a sinusoidal wave microreactor. By simply piled in the central sinusoidal microgroove, CrVPO catalysts with four supports (α-Al_2O_3, γ-Al_2O_3, ZSM-5(50), ZSM-5(80)) were screened and the optimal CrVPO/γ-Al_2O_3 was selected to obtain the optimal reaction conditions by conditional experiments. The optimal result showed that under a tiny catalyst dose of 0.03 g and the optimal feed molar ratio of 1:5:6:12 (MP:H_2O: NH_3:O_2), the best MP conversion and CP selectivity at 480 °C reached 71.5% and 93.7%, respectively. The highest space-time yield of 1724−77 082 $g_{CP}kg_{cat}^{-1}h^{-1}$, to our best knowledge, was achieved, which was 1.9−85 times of the best result reported by a traditional fixed-bed reactor in 2016.[23] Heat intensification was with good control in the sinusoidal wave microreactor and the temperature at the central reaction site varied within ±1 °C for a typical 5-h experiment. The ammoxidation reaction could run stably in the microreactor for at least 50 h with the CP yield remaining 56% ∼ 68%. The results provided a promising approach for ammoxidation reaction to synthesis cyano-containing compounds efficiently and safely.

■ ASSOCIATED CONTENT

Supporting Information

The Supporting Information is available free of charge at https://pubs.acs.org/doi/10.1021/acsomega.2c00039.

N_2 adsorption−desorption isotherms of CrVPO loaded with α-Al_2O_3, γ-Al_2O_3, ZSM-5(50) and ZSM-5(80) by impregnation method; Effects of the immersion time, catalyst particle size, molar ratio of MP to ammonia and molar ratio of MP to oxygen on the CP synthesis (PDF)

■ AUTHOR INFORMATION

Corresponding Author

Xiao Chen − *Key Laboratory of General Chemistry of the National Ethnic Affairs Commission, Southwest Minzu University, Chengdu, Sichuan 610225, China; Key Laboratory of Pollution Control Chemistry and Environmental Functional Materials for Qinghai-Tibet Plateau of the National Ethnic Affairs Commission, Southwest Minzu University, Chengdu, Sichuan 610225, China; Microfluidic Synthesis and Separation Laboratory, College of Chemistry and Environment, Southwest Minzu*

Table 2. Comparison of the Catalytic Ammoxidation from MP to CP among Different Investigations

reactor	m_{cat}	τ	X_{MP}	S_{CP}	Y_{CP}	STY_{CP}	ref
FBR	3 g	1.7 s	∼65%	∼100%	∼65%	38−498 $g_{CP}/(kg_{cat}.h)$	15
FBR	3 g	1.7 s	∼20%	∼100%	∼20%	45−153 $g_{CP}/(kg_{cat}.h)$	16
FBR	5 g	2.8 s	∼90%	∼65%	∼58%	13−266 $g_{CP}/(kgcat·h)$	18
FBR	1 g	/	∼100%	∼70%	∼69%	/	19
FBR	1 g	0.37 s	∼100%	∼70%	∼70%	138−440 $g_{CP}/(kg_{cat}.h)$	20
FBR	1 g	/	∼75%	∼66%	∼50%	/	21
FBR	1 g	/	∼100%	∼85%	∼85%	/	22
FBR	1 g	0.3 s	∼100%	∼86%	∼86%	500−900 $g_{CP}/(kg_{cat}.h)$	23
FBR	1 g	/	∼69%	∼98%	∼67%	/	24
MR	0.03 g	0.001−0.005 s	∼71%	∼97%	∼70%	1724−77 082 $g_{CP}/(kg_{cat}.h)$	this work

https://doi.org/10.1021/acsomega.2c00039
ACS Omega 2022, 7, 8980−8987

University, Chengdu, Sichuan 610041, China; orcid.org/0000-0003-2057-4290; Email: chenxiao@swun.edu.cn

Authors

Meixiu Wei − *Key Laboratory of General Chemistry of the National Ethnic Affairs Commission, Southwest Minzu University, Chengdu, Sichuan 610225, China; Key Laboratory of Pollution Control Chemistry and Environmental Functional Materials for Qinghai-Tibet Plateau of the National Ethnic Affairs Commission, Southwest Minzu University, Chengdu, Sichuan 610225, China*

Haoran Ma − *Microfluidic Synthesis and Separation Laboratory, College of Chemistry and Environment, Southwest Minzu University, Chengdu, Sichuan 610041, China*

Qilin Lu − *Microfluidic Synthesis and Separation Laboratory, College of Chemistry and Environment, Southwest Minzu University, Chengdu, Sichuan 610041, China*

Da Ruan − *Microfluidic Synthesis and Separation Laboratory, College of Chemistry and Environment, Southwest Minzu University, Chengdu, Sichuan 610041, China*

Zhengdong Ma − *Microfluidic Synthesis and Separation Laboratory, College of Chemistry and Environment, Southwest Minzu University, Chengdu, Sichuan 610041, China*

Complete contact information is available at: https://pubs.acs.org/10.1021/acsomega.2c00039

Notes

The authors declare no competing financial interest.

■ ACKNOWLEDGMENTS

This work was supported by the Project of National Natural Science Foundation of China (No. 21406183) and Graduate Innovation Project of Southwest Minzu University (CX2020SZ15). The authors thank Dr. Changjun Liu from Sichuan University for his help with the BET characterization of catalysts and Ms. Juan Li from Ceshigo Research Service (www.ceshigo.com) for the EDS characterization of catalysts. The authors are grateful to Dr. Tao Dai from Southwest Minzu University for fruitful discussions regarding the catalyst characterization analyst.

■ REFERENCES

(1) Rao, K. N.; Gopinath, R.; Prasad, P. S. S. Highly Selective Molybdenum Phosphate Catalyst for the Ammoxidation of 2−Methylpyrazine to 2−Cyanopyrazine. *Green. Chem.* **2001**, *3* (1), 20−22.

(2) Narasimha Rao, K.; Lingaiah, N.; Suryanarayana, I.; Sai Prasad, P. S. A Comparison of Structure and Catalytic Functionality of 12−Molybdophosphoric Acid and Its Ammonium Salt in the Ammoxidation of 2−Methylpyrazine to 2−Cyanopyrazine. *Catal. Lett.* **2003**, *90*, 31−38.

(3) Lankhuyzen, S. P.; Florack, P. M.; Van Der Baan, H. S. The Catalytic Ammoxidation of Propylene over Bismuth Molybdate Catalyst. *J. Catal.* **1976**, *42*, 20−28.

(4) Hu, Y.; Zhao, F.; Wei, F.; Jin, Y. Ammoxidation of Propylene to Acrylonitrile in a Bench-Scale Circulating Fluidized Bed Reactor. *Chem. Eng. Process.* **2007**, *46*, 918−923.

(5) Brazdil, J. F. Designing Multifunctionality into Single Phase and Multiphase Metal-Oxide-Selective Propylene Ammoxidation Catalysts. *Catalysts.* **2018**, *8* (3), 103.

(6) Braga, E. R.; Braga, R. R.; Pontes, L. A. M. Technical and Economic Analysis for the Production of Acrylonitrile from Crude Glycerol. *Chem. Eng. Technol.* **2021**, *44* (12), 2228−2235.

(7) Osipova, Z. G.; Sokolovskii, V. D. Influence of Ammonia on Propane Oxidation over a Gallium−Antimony Oxide Catalyst. *React. Kinet. Catal. Lett. Vol.* **1978**, *9* (2), 193−1981.

(8) Popova, G.Y.; Andrushkevich, T.V.; Chesalov, Y. A.; Plyasova, L.M.; Dovlitova, L.S.; Ischenko, E.V.; Aleshina, G.I.; Khramov, M.I. Formation of Active Phases in MoVTeNb Oxide Catalysts for Ammoxidation of Propane. *Catal. Today.* **2009**, *144*, 312−317.

(9) Woo, J.; Sanghavi, U.; Vonderheide, A.; Guliants, V. V. A Study of M1/M2 Phase Synergy in the MoVTe(Nb, Ta)O Catalysts for Propane Ammoxidation to Acrylonitrile. *Appl. Catal. A: Gen.* **2016**, *515*, 179−189.

(10) Inukai, S.; Ishikawa, S.; Tanabe, T.; Jing, Y.; Toyao, T.; Shimizu, K.-I.; Ueda, W. Thermally Induced Transformation of Sb-Containing Trigonal Mo_3VO_x to Orthorhombic Mo_3VO_x and Its Effect on the Catalytic Ammoxidation of Propane. *Chem. Mater.* **2020**, *32* (4), 1506−1516.

(11) Aliev, S. M.; Sokolovskii, V. D. Ammoxidation of Ethane on Oxide Catalysts. *React. Kinet. Catal. Lett.* **1978**, *9* (1), 91−97.

(12) Bondareva, V. M.; Andrushkevich, T. V.; Aleshina, G. I.; Plyasova, L. M.; Dovlitova, L. S.; Lapina, O. B.; Khabibulin, D. F.; Vlasov, A. A. Ammoxidation of Ethane on V−Mo−Nb Oxide Catalysts. *React. Kinet. Catal. Lett.* **2006**, *87* (2), 377−386.

(13) Liu, X.; Liang, T.; Barbosa, R.; Chen, G.; Toghiani, H.; Xiang, Y. Ammoxidation of Ethane to Acetonitrile and Ethylene: Reaction Transient Analysis for the Co/HZSM-5 Catalyst. *ACS Omega.* **2020**, *5*, 1669−1678.

(14) Liang, T.; Liu, X.; He, Y.; Barbosa, R.; Chen, G.; Fan, W.; Xiang, Y. Highly Selective Sn/HZSM-5 Catalyst for Ethane Ammoxidation to Acetonitrile and Ethylene. *Appl. Catal. A: Gen.* **2021**, *610*, 117942.

(15) Srilakshmi, C.; Lingaiah, N.; Suryanarayana, I.; Prasad, P. S. S.; Ramesh, K.; Anderson, B. G.; Niemantsverdriet, J. W. In Situ Synthesis of Ammonium Salt of 12−Molybdophosphoric Acid on Iron Phosphate and the Ammoxidation Functionality of the Catalyst in the Transformation of 2−Methylpyrazine to 2−Cyanopyrazine. *Appl. Catal. A: Gen.* **2005**, *296* (1), 54−62.

(16) Srilakshmi, C.; Lingaiah, N.; Nagaraju, P.; Sai Prasad, P. S.; Narayana, K. V.; Martin, A.; Lücke, B. Studies on Bulk Metal Phosphate Catalysts for the Ammoxidation of 2−Methylpyrazine. *Appl. Catal. A: Gen.* **2006**, *309* (2), 247−253.

(17) Hong, C.; Li, Y.; Fu, Z.; Zhang, S. Preparation of 2−Cyanopyrazine from 2−Methylpyrazine by Catalytic Ammoxidation over CrVPO Catalyst. *Chin. J. Zhejiang Univ−sc.* **2006**, *11*, 1922−1925.

(18) Srilakshmi, C.; Nagaraju, P.; Sreedhar, B.; Sai Prasad, P. S.; Kalevaru, V. N.; Lücke, B.; Martin, A. Ammoxidation Activity of in Situ Synthesized Ammonium Salt of Molybdophosphoric Acid on $VOPO_4$ Catalysts. *Catal. Today.* **2009**, *141* (3−4), 337−343.

(19) Dhachapally, N.; Kalevaru, V. N.; Brückner, A.; Martin, A. Metal Vanadate Catalysts for the Ammoxidation of 2−Methylpyrazine to 2−Cyanopyrazine. *Appl. Catal. A: Gen.* **2012**, *443−444*, 111−118.

(20) Dhachapally, N.; Kalevaru, V. N.; Martin, A. Ammoxidation of 2−Methylpyrazine to 2−Cyanopyrazine over Nb−V Oxides: Marked Effect of the Nb/V Ratio on the Catalytic Performance. *Catal. Sci. Technol.* **2014**, *4* (9), 3306−3316.

(21) Alshammari, A.; Kalevaru, V. N.; Dhachapally, N.; Köckritz, A.; Bagabas, A.; Martin, A. Nanosize Gold Promoted Vanadium Oxide Catalysts for Ammoxidation of 2−Methylpyrazine to 2−Cyanopyrazine. *Top. Catal.* **2015**, *58* (14−17), 1062−1068.

(22) Radnik, J.; Dhachapally, N.; Kalevaru, V. N.; Sinev, I.; Grünert, W.; Martin, A. Impact of the Outermost Layer of Various Solid Metal Vanadate Catalysts on Ammoxidation of 2−Methyl pyrazine to 2−Cyanopyrazine. *Catal. Commun.* **2015**, *71*, 97−101.

(23) Kalevaru, V.; Dhachapally, N.; Martin, A. Catalytic Performance of Lanthanum Vanadate Catalysts in Ammoxidation of 2−Methylpyrazine. *Catalysts* **2016**, *6* (1), 10.

(24) Al-Shehri, A.; Katabathini, N. Influence of Polyoxometalate Structure in Ammoxidation of 2−Methylpyrazine. *Catal. Commun.* **2018**, *108*, 17−22.
(25) Zhou, F.; Liu, H.; Wen, Z.; Zhang, B.; Chen, G. Toward the Efficient Synthesis of Pseudoionone from Citral in a Continuous−Flow Microreactor. *Ind. Eng. Chem. Res.* **2018**, *57* (33), 11288−11298.
(26) Adiyala, P. R.; Jang, S.; Vishwakarma, N. K.; Hwang, Y.-H.; Kim, D.-P. Continuous−Flow Photo−Induced Decarboxylative Annulative Access to Fused Imidazole Derivatives Via a Microreactor Containing Immobilized Ruthenium. *Green. Chem.* **2020**, *22* (5), 1565−1571.
(27) Guo, W.; Heeres, H. J.; Yue, J. Continuous Synthesis of 5−Hydroxymethylfurfural from Glucose Using a Combination of $AlCl_3$ and HCl as Catalyst in a Biphasic Slug Flow Capillary Microreactor. *Chem. Eng. J.* **2020**, *381*, 122754.
(28) Russo, D.; Tomaiuolo, G.; Andreozzi, R.; Guido, S.; Lapkin, A. A.; Di Somma, I. Heterogeneous Benzaldehyde Nitration in Batch and Continuous Flow Microreactor. *Chem. Eng. J.* **2019**, *377*, 120346.
(29) Zhao, S.; Yao, C.; Zhang, Q.; Chen, G.; Yuan, Q. Acoustic Cavitation and Ultrasound-Assisted Nitration Process in Ultrasonic Microreactors: The Effects of Channel Dimension, Solvent Properties and Temperature. *Chem. Eng. J.* **2019**, *374*, 68−78.
(30) Zhang, C.; Zhang, J.; Luo, G. Kinetic Study and Intensification of Acetyl Guaiacol Nitration with Nitric Acid−Acetic Acid System in a Microreactor. *J. Flow. Chem.* **2016**, *6* (4), 309−314.
(31) Liu, Q.; Qiu, W.; Wu, P.; Yue, H.; Liu, C.; Jiang, W. Low−Temperature Ammonia Oxidation in a Microchannel Reactor with Wall−Loaded X(X = Pt, Pd, Rh, PtPdRh)/TiO_2 Nanotube Catalysts. *Ind. Eng. Chem. Res.* **2019**, *58* (23), 9819−9828.
(32) Lin, J.; Tian, J.; Cheng, X.; Tan, J.; Wan, S.; Lin, J.; Wang, Y. Propane Ammoxidation over MoVTeNb Oxide Catalyst in a Microchannel Reactor. *AlChE J.* **2018**, *64* (11), 4002−4008.
(33) Jiao, Y.; Zhang, J.; Du, Y.; Yao, P.; Wang, J.; Lu, J.; Chen, Y. Hydrogen−Rich Syngas Production by Toluene Reforming in a Microchannel Reactor Coated with Ni/MgO−Al_2O_3 Multifunctional Catalysts. *Ind. Eng. Chem. Res.* **2019**, *58* (43), 19794−19802.
(34) Chen, J.; Song, W.; Xu, D. Compact Steam−Methane Reforming for the Production of Hydrogen in Continuous Flow Microreactor Systems. *ACS Omega.* **2019**, *4* (13), 15600−15614.
(35) Mohammad, N.; Abrokwah, R. Y.; Stevens-Boyd, R. G.; Aravamudhan, S.; Kuila, D. Fischer−Tropsch Studies in a 3D−Printed Stainless Steel Microchannel Microreactor Coated with Cobalt-Based Bimetallic−MCM−41 Catalysts. *Catal. Today.* **2020**, *358*, 303−315.
(36) Zhang, X.; Yu, F.; Zhang, J.; Tang, Z.; Sun, Y. A Novel Cobalt Carbide Catalyst Wall−Coating Method for FeCrAlloy Microchannels Exemplified on Direct Production of Lower Olefins from Syngas. *Ind. Eng. Chem. Res.* **2019**, *58* (51), 22967−22976.
(37) He, L.; Fan, Y.; Luo, L.; Bellettre, J.; Yue, J. Preparation of Pt/γ−Al_2O_3 Catalyst Coating in Microreactors for Catalytic Methane Combustion. *Chem. Eng. J.* **2020**, *380*, 122424.
(38) Behravesh, E.; Eranen, K.; Kumar, N.; Peltonen, J.; Peurla, M.; Aho, A.; Nurmi, M.; Toivakka, M.; Murzin, D. Y..; Salmi, T. Microreactor Coating with Au/Al_2O_3 Catalyst for Gas−Phase Partial Oxidation of Ethanol: Physico−Chemical Characterization and Evaluation of Catalytic Properties. *Chem. Eng. J.* **2019**, *378*, 122179.
(39) Jannesar, E. A.; Hamzehpour, H. Acoustic Tweezing of Microparticles in Microchannels with Sinusoidal cross Sections. *Sci. Rep.* **2021**, *11*, 17902.

NOTE ADDED AFTER ASAP PUBLICATION

This paper was published ASAP on March 2, 2022, with an error in the Abstract image. The corrected version was posted on March 15, 2022.

https://doi.org/10.1021/acsomega.2c00039
ACS Omega 2022, 7, 8980−8987